TITLE : Improving Photoluminescence Emissions and Photostability of Dye/MgAl-Layered Double Hydroxide Nanohybrids

مشخصات مقاله : چاپ شده/ انگليسي/ مقاله كامل - ARTICLE

گروه علمي : علوم پايه	حوزه فعاليت : نانو، فناوري	داراي رويكرد اسلامي: خير

مشخصات مجله محل چاپ :

شماره مجله : ۲۰۰۰۰۳۴۱۹	ISSN: 2365-6549	EISSN:

TITLE : ChemistrySelect

محل انتشار :	زبان مجله:	دوره انتشار:
(No)جندمين شماره : -- (Vol)جندمين سري انتشار :۸	سال انتشار : تير۱۴۰۲ ميلادي : Jul۲۰۲۳	شماره صفحه : ۱ تا ۷

نمايه هاي مجله :۲۰۰۰۰۳۴۱۹

نوع نمايه مجله	IF	MIF	AIF	Q	كد	شرح موضوع	JCR	رتبه ارزيابي
ISI	IF=2/1	MIF=3/2	AIF=6/9	Q=3	۱۵۵	CHEMISTRY MULTIDISCIPLINARY SCIE -	۶۷/۶۳	
SCOPUS	IF=	MIF=	AIF=	Q=2	۶۲۰	Chemistry (miscellaneous)		
SCOPUS	IF=	MIF=	AIF=		۱	Scopus		

همكاران مقاله :

چندمين همكار	نوع همكار	نام همكار	درصد همكاري	مستخرج از تز	دانشكده مرتبط	گروه آموزشي مرتبط	سازمان مرتبط	رديف وابستگي
۱	هيات علمي خارج از دانشگاه	Zolfaghar Rezvani		خير				۱
۲	دانشجوي خارج از دانشگاه	Leila Jafari Foruzin		خير				۱
۳	هيات علمي دانشگاه	نجاتي كاميلا		خير	علوم پايه	شيمي		۱

ChemistrySelect

Research Article
doi.org/10.1002/slct.202300629

Chemistry Europe
European Chemical Societies Publishing

www.chemistryselect.org

Improving Photoluminescence Emissions and Photostability of Dye/MgAl-Layered Double Hydroxide Nanohybrids

Zolfaghar Rezvani,*[a] Leila Jafari Foruzin,[a] and Kamellia Nejati[b]

The purpose of this study was the preparation of layered double hydroxide (LDH) -based nanohybrids with improved photoluminescence emission and high photostability. The anion exchange-based microwave method was applied for the intercalation of mordant orange 1 into MgAl-LDH. The prepared organic-inorganic nanohybrid was confirmed by X-ray diffraction, thermal gravimetric analysis (TGA), inductively coupled plasma spectrometry (ICP), and infrared spectra (FT-IR). Also, the morphology of the obtained sample was investigated using the field emission-scanning electron microscopy (FE-SEM) method. In the MgAl-LDH interlayer space, a tilted orientation and bilayer arrangement were predicted for the mordant orange 1 anions. Compared with the pure mordant orange 1, the MgAl-LDH/mordant orange 1-MA (prepared using the microwave-based anion exchange method) has improved photoluminescence emission with high Photostability. These findings supply a new approach for designing photoluminescence materials that potentially apply to optical devices with high Photostability.

Introduction

The layered double hydroxides (LDHs) have several advantages such as unique structure, large intercalated anions within interlayer spaces, and uniform distribution of metals in the layered structure which make the LDHs significant layered materials.[1] LDHs contain the general formula as follows: $M^{3+}_x [M^{2+}_{1-x} (OH)_2]^{x+} [A_{x/n}]^{n-}.nH_2O$, where trivalent metal cations (M^{3+}) can be metals such as Fe^{3+}, Al^{3+}, Mn^{3+}, or Cr^{3+}, e.g. and divalent metal cations (M^{2+}) was Zn^{2+}, Mg^{2+}, Co^{2+} or Mg^{2+}.

The interlayered anion was shown with A^{n-}, which can be an organic or inorganic anion.[2] Also, at the interlayer of LDHs, the water molecules create hydrogen bonds with hydroxyl groups that surround octahedrally the metal centers. The x was equated with the molar ratio of $M^{3+}/(M^{2+}+M^{3+}$.[3] The positive charge, which was created using the substitution of some M^{2+} by M^{3+} was balanced using intercalated anions.[4] The LDHs can be prepared using the co-precipitation method,[5] hydrothermal method,[6] ultrasonic-assisted method[7] or microwave-assisted method.[8] Among several anions which were applied as the interlayer molecules, dye anions are considered exciting guest species due to their host-guest interaction may provide unique physicochemical and photoluminescence properties.[9] Lately, different intercalated methods such as ion exchange,[9b] co-precipitation,[10] hydrothermal,[11] and microwave[12] have been studied and applied to the synthesis of LDH nano-hybrids. These methods are broadly applied to the preparation of different nanohybrids based on organic/LDH, such as Tartrazine,[13] Allura Red AC,[14] Direct yellow 50,[15] Acid Red 27,[16] Cyanine dye[9b] and Orange G.[17] Among the mentioned methods, the co-precipitation and anion exchange methods were applied widely for the intercalation of anions. However, one of the disadvantages of these methods is that it takes a long time to perform the reaction. Also, generally, the LDHs as the precursor for the anion exchange method were prepared using the co-precipitation method, which necessitated a long time of 12–18 h for the synthesis of LDH at the first step.[18] In addition, the direct intercalation of dye into the interlayer space of LDHs using anion exchange or co-precipitation method can be a problem due to the uncontrollable intercalation of dye or attaching of anion to the surface of the LDHs at high concentrations of dye, which can be quenched physical properties such as photoluminescence emissions.[19] To overcome the problems of aggregation, the researchers used the co-intercalation method and adding the surfactant during the preparation process.[20] Surfactants such as sodium fluorescein or alkyl were used to modify physicochemical properties at LDH nanohybrids using co-intercalation and anion exchange methods.[21] This method can reduce the fluorescence quenching by decreasing the aggregation of anions at the interlayer of LDHs. Nevertheless, decreasing the aggregation at the intercalated process is challenging for researchers.

Recently, intercalation using microwave- assistant method has received more attention.[12] The advantage of this process is decreasing the time of reaction. Intercalation using microwave-assistant method can be used as a method to control the dye molecules inside the LDH layers and improve the fluorescence properties of the nanohybrid. Our research group intercalated the mordent orange into ZnAl-LDH[22] but at the photoluminescence devices, Photostability of prepared nanohybrids is

[a] Prof. Z. Rezvani, Dr. L. Jafari Foruzin
Department of Chemistry, Faculty of Basic Sciences, Azarbaijan Shahid Madani University, 5375171379 Tabriz, Iran
E-mail: z_rezvani@yahoo.com

[b] Dr. K. Nejati
Department of Chemistry, Payame Noor University, P.O.BOX 19395—3697, 5174875651 Tehran, Iran

a key point for increased efficiency of the device. On the other hand, the Photostability of azoic dyes such as mordant orange 1 is very poor under UV light. So, the use of transition metals which increase the Photostability is very important. At ZnAl-LDH nanohybrids due to present Zn, the band gap energy was decreased,[23] so, these nanohybrids can be degraded by the intercalated azoic dye. At ZnAl-LDH nanohybrids suffers from poor Photostability compared with MgAl-LDH.

This research aims to prepare a nanohybrid with improved photoluminescence (PL) properties with high Photostability using a microwave-based anion exchange method as a safe and green method to reduce the reaction time and increased the Photostability at photoluminescence materials. The prepared nanohybrids were characterized by XRD, FT-IR, TGA, CHN, ICP, and FE-SEM techniques. The resulting nanohybrids have improved PL emission with high Photostability compared with the pure dye and MgAl-LDH/dye synthesized using the co-precipitation-based anion exchange method (MgAl-LDH/dye-MA). The prepared nanohybrids possess advantages over pure dye at photoluminescence devices.

Results and Discussion

The X-ray diffraction (XRD) patterns of prepared materials are presented in Figure 1, as shown in Figure 1(a), the XRD pattern of the MgAl-LDH phase was characteristic of an LDH structure, which was indexed $R\bar{3}m$ space group at rhombohedral symmetry with a hexagonal system.[24] The space of interlayer at LDHs was related to the position of (003) planes (first peak).

The position of (003) diffraction peak at pure MgAl-LDH at 2θ about 10.4° can achieve an interlayer spacing of LDH layers of about 8.5 Å. After intercalation of anionic dye into the interlayers of MgAl-LDH, the (003) peak was shifted to 3.3°, and the basal space was estimated at 26.7 Å. These results show that after intercalation, the distance of interlayers at LDHs was increased, due to the intercalation of mordant orange 1 dye (Figure 1(b)). Also, about MgAl-LDH/dye-A which the dye anion was intercalated using a co-precipitation-based anion exchange method, the distance of interlayers was calculated at about 24.5 Å ($2\theta = 3.6°$) but anions which adsorbed on the LDH appeared as an impurity as shown at Figure 1(c).

The lattice parameters of "c" and "a" were calculated as follows:

$$c = 3\ d_{003} \quad (1)$$

$$a = 2\ d_{110} \quad (2)$$

The lattice parameters of "a" and "c" for MgAl-LDH were calculated at about 3.0 Å and 25.5 Å, respectively. The lattice parameter of "a" for MgAl-LDH/dye-MA was estimated at 3.1 Å which was similar to the MgAl-LDH. The obtained data confirm that the cationic order at LDHs before and after intercalation of dye was not changed. However, the calculated "c" for MgAl-LDH/dye-MA was estimated at 80.1 Å. Also, at the XRD pattern of the MgAl-LDH/dye-MA (Figure 1(b)), the XRD pattern has a single LDH phase. Besides, the increase in the interlayer space appeared by shifting the position of (003) peak toward low 2θ. The calculated value for the distance of the interlayer was estimated from d_{003}, which is the sum of the thickness of the layer and gallery height. Based on that, the thickness of the MgAl-LDH layer was calculated at 4.8 Å,[25] so for MgAl-LDH/dye-MA, the gallery height is about 21.9 Å. The length of the dye anion was calculated at about 12.68 Å (scheme 1) and this value is smaller than the value of gallery height. Also, the twice dye length is higher than that of the gallery height. So, as shown in Scheme 2, the azoic dye anions intercalated into LDH interlayer as a bilayer.[26]

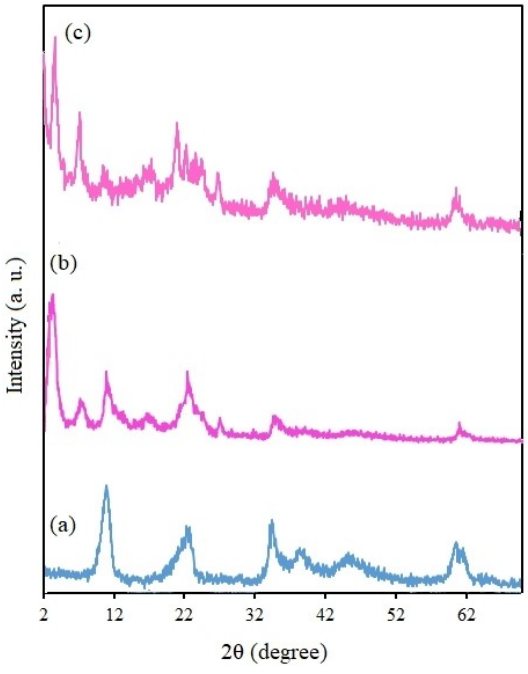

Figure 1. XRD patterns of (a) MgAl-LDH (b) MgAl-LDH/dye-MA, and (c) MgAl-LDH/dye-A.

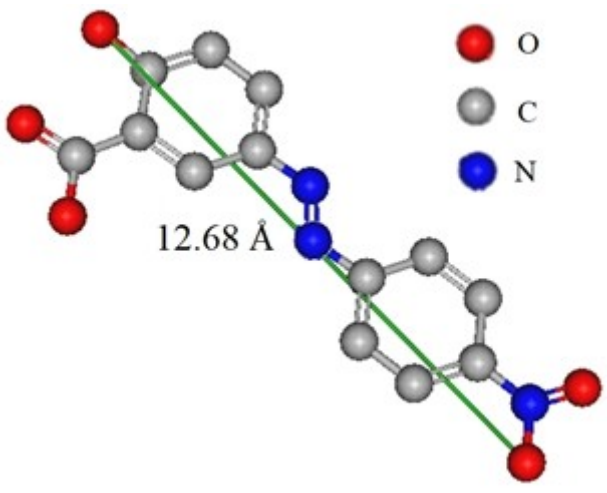

Scheme 1. 3D structure of mordant orange 1.

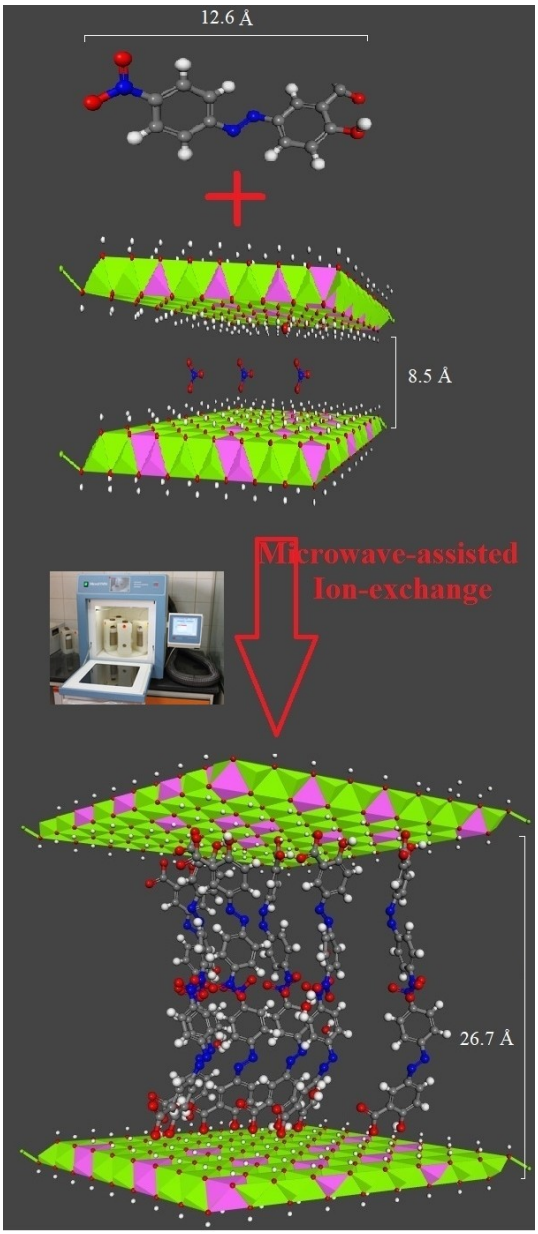

Scheme 2. Structural model of MgAl-LDH/dye-MA.

By applying the Debye-Scherrer equation (Eq. (3)) on the XRD patterns, the average crystallite size (D) of the MgAl-LDH, MgAl-LDH/dye-MA, and MgAl-LDH/dye-A can be calculated as:

$$D = 0.9\,\lambda/\beta\cos\theta \quad (3)$$

where D is the crystallite size (in nm), " λ " is the wavelength of the X-ray used (in nm), " β " is the full width at half maximum (FWHM-in radian), and " θ " is the Bragg diffraction angle.[27] The average crystallite size, D, is calculated as: 12.3, 8.4, and 14.4 nm for MgAl-LDH, MgAl-LDH/dye-MA, and MgAl-LDH/dye-A, respectively.

Figure 2(a, b, and c) present FT-IR spectra of mordant orange 1(dye), MgAl-LDH, and MgAl-LDH/dye-MA nanoparticles.

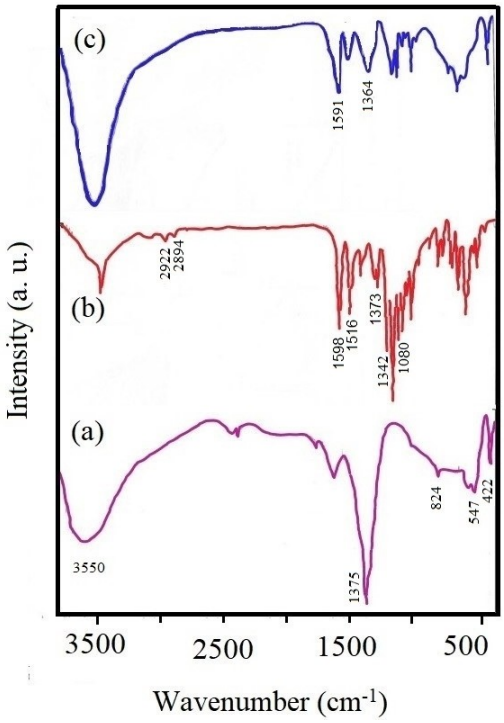

Figure 2. FT-IR spectra (a) MgAl-LDH, (b) dye, and (c) MgAl-LDH/dye-MA.

As shown in Figure 2(a), the broadband at 3550 cm^{-1} can be associated with O–H stretching vibration of layers, and H_2O at interlayer space. The ν_3 stretching vibration of intercalated NO_3 appeared at 1375 cm^{-1}. Also, a weak peak was observed at 824 cm^{-1} that can be associated with the ν_2 stretching mode of nitrate anion.[28] These peaks disappeared after the intercalation of dye in the interlayer of LDHs. These indicated the intercalation of azoic dye into the LDH interlayer.[29] Also, the bending vibration of M–OH was reported at 547 cm^{-1}, and the M–O–M peak appeared at 422 cm^{-1}.[30] In Figure 2(b), the stretching vibration of H–C is observed at 2894 and 2922 cm^{-1}. The characteristic peak of O–H appeared at 3400 cm^{-1}. The peaks at 1373 and 1598 cm^{-1} were attributed to asymmetric and symmetric vibrations of the COOH group.[31] The stretching vibration of aromatic C–C was reported at 1516 cm^{-1}.[32] Also, the C–O stretching vibration was reported at 1080 cm^{-1}. Besides, the peak corresponding to the NO_2 group appeared at 1342 cm^{-1}.[33] After intercalation of anionic dye into MgAl-LDH (Figure 2(c), the asymmetric and symmetric vibrations of the COOH slightly shifted, and appeared at 1364 and 1591 cm^{-1}, respectively due to hydrogen interaction between COOH···H–O–M (the metal can be bivalent or trivalent).[34] Also, at MgAl-LDH/dye-MA the intensity of the OH peak is higher than that of MgAl-LDH. It can be attributed to the absorbed H_2O by KBr, and more hydrogen bonding interactions between OH groups of layers and dye anion which is used to make KBr tablets.

Figure 3(a) and (b) reported the morphology of MgAl-LDH after and before the dye intercalation. Both the prepared LDHs have plate-like morphology, and the thickness of LDHs at MgAl-

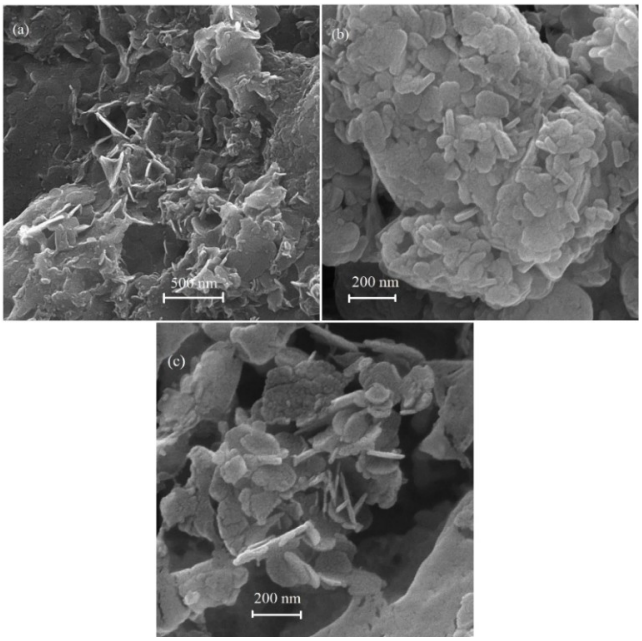

Figure 3. FE-SEM graphs of (a) MgAl-LDH, (b) MgAl-LDH/dye-MA, and MgAl-LDH/dye-A.

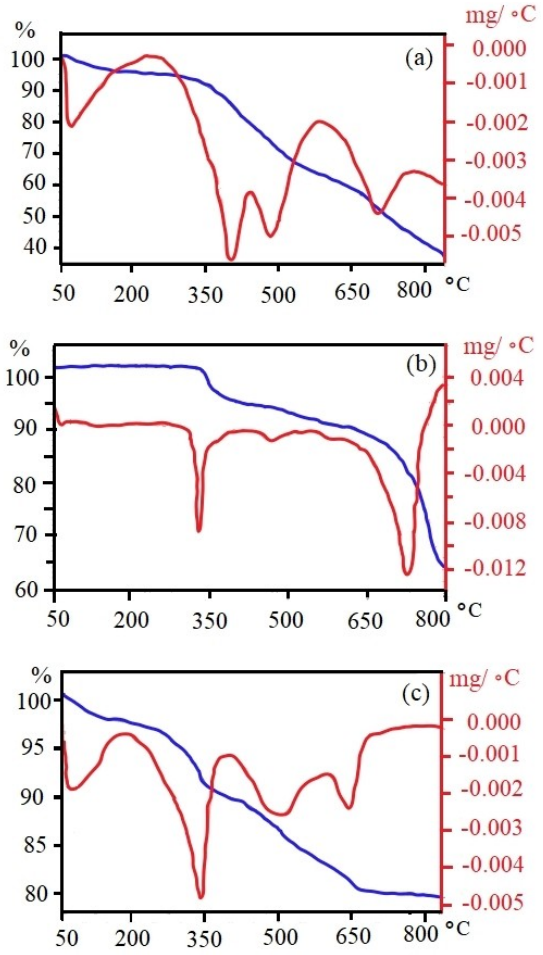

Figure 4. TGA and DTG curves of (a) MgAl-LDH/dye-MA (b) dye, and (c) MgAl-LDH.

LDH and MgAl-LDH/dye-MA were estimated 20.9 and 26.7 nm, respectively(by using Image J software). Besides, the intercalation of dye into the MgAl-LDH using microwave-based anion-exchange method has not changed the structure and morphology of MgAl-LDH that confirm the MgAl-LDH/dye-MA nanohybrid has been prepared successfully. Besides, unlike the plates of MgAl-LDH, at MgAl-LDH/dye-MA, the plates were ordered and smooth. As reported in Figure 3(c), after intercalation using a co-precipitation-based anion-exchange method, the aggregation clearly can be seen, and the plates were disordered.

The thermal gravimetric (TG) and derivative thermal gravimetric (DTG) analyses for the MgAl-LDH/dye-MA, pure dye, and MgAl-LDH are shown in Figure 4(a), (b), and (c). As shown in Figure 4(a), the four steps were exhibited for the thermal behavior of MgAl-LDH/dye-MA. In the first step (50–215 °C), the physically adsorbed water was vaporized (5%). At the second step, from 215–447 °C, the partial dehydroxylation of the nanohybrid occurred, and this value was estimated at 17%. The decomposition was followed by the loss of organic materials at the third step 447–597 °C (14.6%). The more decomposition process events (597–845 °C) due to more dehydroxylation of MgAl-LDH/dye-MA (25.9%). Also, the corresponding DTG peaks for the first, second, third, and fourth steps appeared at 65, 410, 485, and 695 °C, respectively. As shown in Figure 4(b), under the calcination process from 50–800 °C, during the third step the pure dye was degraded. In the range, of 50–375 °C (first step), the evaporation of adsorbed water and dehydroxylation occurred (5.63%). In the second step, the decomposition of organic materials from 375–540 °C was reported (4.37%). In the last step (540–800 °C), the decomposition of remaining organic materials and more dehydroxylation were seen (28.22%). The DTG peaks were reported at 330, 460, and 730 °C for the first, second, and third steps, respectively. In the case of MgAl-LDH, as shown in Figure 4(c), the first thermal behavior occurred from 50–200 °C. This step is attributed to the vaporization of the adsorbed and interlayer water molecules (3.75%). In the next step (200–395 °C), the dehydroxylation of LDH occurred (8.75%).[35] The thermal decomposition takes place by burning organic molecules at 395–605 °C (8.25%). At the fourth step, from 605–830 °C, the burning of remaining organic molecules occurred (3.25%). As shown in Figure 4(c), the corresponding DTG peaks were observed at 65, 350, 500, and 650 °C for the first, second, third, and fourth steps.

All weight losses at MgAl-LDH/dye-MA during thermal treatment were reported at about 62.5%, and pure dye and MgAl-LDH were degraded at about 38% and 23.5%. So, using the difference between weight losses at MgAl-LDH/dye-MA, and MgAl-LDH, we can estimate that weight loss contributed from the dye intercalated in interlayers about 39%. This analysis result was in agreement with ICP and CHN data as presented in Table 1, which can be calculated from the molecular formula of the composite.

Table 1. Elemental chemical analyses for MgAl-LDH/dye-MA, and MgAl-LDH/dye-A nanohybrids.

Sample	Mg (%)	Al (%)	C (%)	H (%)	N (%)	Composition
MgAl-LDH/dye-MA	19	7	33	4	6	$[Mg_3Al(OH)_8](O_2NC_6H_4N_2C_6H_3(OHCO_2H)_{0.5}\cdot 0.8H_2O$

To study the optical properties of prepared MgAl-LDH/dye-MA, its emission spectrum was reported. The result was compared with MgAl-LDH/dye-A and pure dye photoluminescence (PL) curves, as shown in Figure 5. All three samples were excited at the wavelength of about 416 nm. For the PL study, 0.001 gr of samples were dispersed in 10 mL water. The PL curves were obtained at room temperature. The emission peaks for MgAl-LDH/dye-A, MgAl-LDH/dye-MA, and pure dye appeared at 587.5, 560, and 555 nm, respectively. The obtained data demonstrate that the intensity of the fluorescence emission at MgAl-LDH/dye-MA is significantly higher than that of pure dye. Also, about MgAl-LDH/dye-MA, a small peak appeared at 625 nm due to the transformation of energy from mordant orange 1 to Mg.[36] MgAl-LDH/dye-A shows negligible emission, which emission has a red-shift in comparison with the pure dye. This red shift and fluorescence quenching were due to the aggregation of dye at the intercalation process.[37] But at MgAl-LDH/dye-MA the PL intensity is significantly higher than that of pure dye. Also, about MgAl-LDH/dye-MA, the red-shift was decreased that shows the aggregation was decreased. These results confirm that the microwave-based anion exchange method can be a suitable method for improving photoluminescence emission.

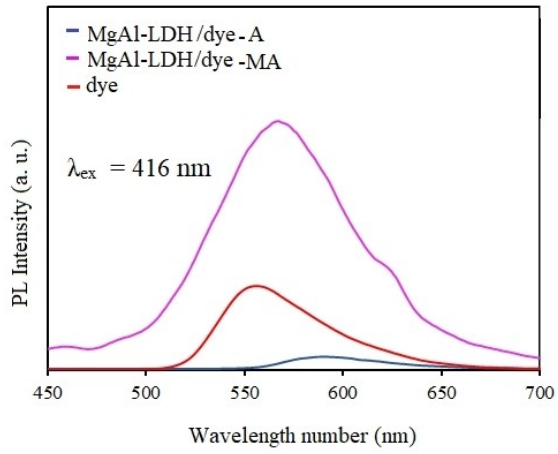

Figure 5. Photoluminescence emission of MgAl-LDH/dye-MA, MgAl-LDH/dye-A, and pure dye.

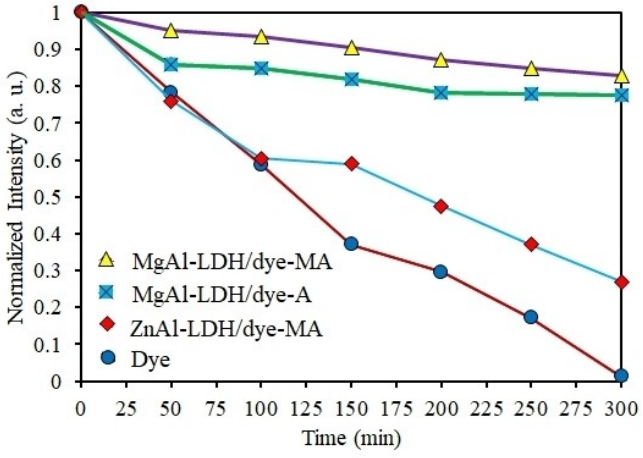

Figure 6. Photostability of Mordent orange dye, and dye/MgAl-LDH.

The Photostability is an important factor in the fluorescence device. This is due to the limitation of detection which consequently decreased the intensity of reversible fluorescence under light. So, to study the optical stability of the prepared nanohybrid, the PL emission intensity of the Mordent orange dye, and MgAl-LDH/dye-MA, MgAl-LDH/dye-A have been investigated after exposure of the sample under the UV light. Also, for comparison the Photostability of ZnAl-LDH/dye-MA which was prepared under the same condition and microwave-based anion exchange method, ($[Zn_3Al(OH)_8](O_2NC_6H_4N_2C_6H_3(OHCO_2H)_{0.5}\cdot 0.8H_2O$) was investigated. The exciting wavelength for PL emission was 400 nm. Figure 6 presents the fluorescence emission curve during dye degradation times. The data confirm that during 300 min, when the sample was exposed to UV irradiation due to early degradation, the intensity of the PL emission in the pure Mordent orang dye signally decreases. But at the MgAl-LDH/dye-MA, slight degradation within the 200 min was reported, then after 200 min the intensity of the PL emission remains constant. Also, at MgAl-LDH/dye-A the Photostability is poor than that MgAl-LDH/dye-MA. This can be attributed to the early degradation of dye which is absorbed on the surface of LDH as reported in Figure 1(c). Also, at ZnAl-LDH/dye-MA the Photostability is very poor due to the low band gap energy of ZnAl-LDH.[23,38] Therefore, the Photostability was improved at the intercalated MgAl- LDH/dye-MA sample and the intensity of normalized fluorescence was higher compared with the pure dye, MgAl- LDH/dye-A and ZnAl-LDH/dye-MA.

Conclusions

An ordered MgAl-LDH/dye-MA with high Photostability was successfully synthesized by the microwave-based anion-exchange method. The reported data from thermal gravimetric analysis (TGA), X-ray diffraction, and FT-IR spectroscopy show that the mordant orange 1 dye successfully has been intercalated into the MgAl-LDH interlayer. The optical properties of MgAl-LDH/dye-MA were investigated using PL spectra. The PL emission results show improved photoluminescence emission. In the MgAl-LDH/dye-MA, due to the decreased time of the intercalation process, it can decrease the aggregation of dye

compared with the co-precipitation-based anion exchange method. Also, the Photostability of MgAl-LDH/dye-MA was improved compared with pure dye, MgAl-LDH/dye-A due to the complete interaction of dye into the LDH interlayer. So, the microwave-based anion-exchange method is an alternative method compared to the co-precipitation-based anion-exchange method. The obtained results may present essential information on how we can decrease the photoluminescence quench phenomena during the intercalation process.

Experimental Section

General

X-ray diffraction (XRD) patterns of prepared materials were obtained at diffraction angles 2–70° using a Bruker AXS model-D8 with Cu Kα radiation. To study the morphology of samples, field emission-scanning electron microscopy (FE-SEM) was applied by the TESCAN device – VEGA II. Also, the average LDH thickness was measured by Image J software. Fourier transform infrared (FT-IR) spectrum was recorded by Perkin-Elmer spectrophotometer at wavenumber from 400 to 3700 cm^{-1}, using a KBr disk. The thermogravimetric analysis of prepared materials was investigated by the Linseis STA PT-1000 instrument with a nitrogen atmosphere and a heating rate of 10 °C.min^{-1}. The PL emission was measured using an FP-6200 spectrophotometer. The Shimadzu - ICPS-7500 was used for the study of inductively coupled plasma spectrometry (ICP).

Preparation of MgAl-LDH

The MgAl-LDH was prepared using the co-precipitation method under ultrasound waves. 0.002 M (0.042 g) of $Al(NO_3)_2.9H_2O$ solution and 0.006 M (0.15 g) of $Mg(NO_3)_2.6H_2O$ solution were mixed and placed in a round balloon of 100 mL. Then the solution was placed in a water bath under an N_2 atmosphere and ultrasound waves with an intensification frequency of about 40000 Hz. The ultrasonic power was about 305 W. Then, under ultrasound waves, the pH of the clear solution reached 10 using sodium hydroxide solution 0.1 M. The obtained colloid was kept under ultrasound waves for 70 min. The sample was centrifuged and washed with deionized water several times and dried overnight under a vacuum to produce MgAl-LDH-NO_3.

Synthesis of MgAl-LDH/mordant orange 1 nanohybrid

The mordant orange 1 (azoic dye) was intercalated into MgAl-LDH by the anion exchange technology. Firstly 0.002 M (0.057 g) mordant orange 1 was dispersed in 100 mL water, and the pH of the solution was adjusted to 10 by using sodium hydroxide solution (1 M). In the next step, 2.0 g of dried MgAl-NO_3-LDH, which was freshly synthesized, was added to a dye solution under a nitrogen atmosphere at 80 °C. The mixture was transformed into a Teflon vessel and was aged under microwave waves with a power MWI of about 50 W at 80 °C for 4 h. The resulting product MgAl- LDH/ mordant orange 1 was filtered and three times washed using pure water. The obtained sample was named MgAl-LDH/dye-MA. Also, the MgAl-LDH/dye nanohybrids were prepared using the co-precipitation-based anion exchange method. The conditions of preparation are similar, except that in the aging step, the sample is stirred for 24 h at 80 °C (instead of microwave waves). The obtained powders were labeled as MgAl-LDH/dye-A.

Author Contributions

Zolfaghar Rezvani: Supervision, Conceptualization, Resources, review & editing, Data curation, Project administration, Writing – review & editing. Leila Jafari Foruzin: Methodology, Validation, Investigation, Writing – original draft, Visualization. Kamellia Nejati: Validation, Resources, Conceptualization, Writing – review & editing.

Acknowledgements

The Azarbijan Shahid Madani University financially supported this research [Grant No. 1-155/1400].

Conflict of Interests

The authors declare no conflict of interest.

Data Availability Statement

The data that support the findings of this study are available from the corresponding author upon reasonable request.

Keywords: Azoic dye · Intercalation · Nanohybrid · Photoluminescence Emission · Photostability

[1] L. Mohapatra, K. Parida, *J. Mater. Chem. A* **2016**, *4*, 10744–10766.
[2] a) M. Zubair, I. Ihsanullah, H. A. Aziz, M. A. Ahmad, M. A. Al-Harthi, *Bioresour. Technol.* **2021**, *319*, 124128; b) D. Zhou, P. Li, X. Lin, A. McKinley, Y. Kuang, W. Liu, W.-F. Lin, X. Sun, X. Duan, *Chem. Soc. Rev.* **2021**, *50*, 8790–8817.
[3] a) H. Kaur, S. Singh, B. Pal, *Korean J. Chem. Eng.* **2021**, *38*, 1248–1259; b) S. Radhakrishnan, K. Lauwers, C. V. Chandran, J. Trebosc, J. A. Martens, F. Taulelle, C. E. Kirschhock, E. Breynaert, *Chem. Eur. J.* **2021**, *27*, 15944–15953.
[4] K. N. Dhakal, G. M. Aryal, H. S. Adhikari, R. Adhikari, *J. Nepal Chem. Soc.* **2021**, *42*, 39–44.
[5] a) O. D. Pavel, A.-E. Stamate, E. Bacalum, B. Cojocaru, R. Zăvoianu, V. I. Pârvulescu, *Catal. Today* **2021**, *366*, 227–234; b) Z. Jiang, J. Wu, X. Liu, H. Yu, C. Jiao, J. Shen, Y. Pei, *New J. Chem.* **2021**, *45*, 14580–14588.
[6] a) C. Huang, J. Nie, Z. Xu, X. Zhang, J. Tang, B. Wang, J. Huang, C. Du, J. Chen, *Int. J. Hydrogen Energy* **2021**, *46*, 12992–13000; b) T. Kokulnathan, T.-J. Wang, F. Ahmed, T. Alshahrani, *Chem. Eng. J.* **2023**, *451(3)*, 138884.
[7] a) T.-J. Wang, X. Liu, Y. Li, F. Li, Z. Deng, Y. Chen, *Nano Res.* **2020**, *13*, 79–85; b) S. Yusuf, A. Moheb, M. Dinari, *Res. Chem. Intermed.* **2021**, *47*, 1297–1313.
[8] a) C. Qiao, Y. Zhang, Y. Zhu, C. Cao, X. Bao, J. Xu, *J. Mater. Chem. A* **2015**, *3*, 6878–6883; b) D. Chen, Y. Li, J. Zhang, J.-z. Zhou, Y. Guo, H. Liu, *Chem. Eng. J.* **2012**, *185*, 120–126; c) J. Fang, M. Li, Q. Li, W. Zhang, Q. Shou, F. Liu, X. Zhang, J. Cheng, *Electrochim. Acta* **2012**, *85*, 248–255.
[9] a) Y. Liu, Y. Gao, Z. Zhang, Q. Wang, *Chemosphere* **2021**, *277*, 130370; b) R. Sato, S. Machida, M. Sohmiya, Y. Sugahara, R. Guégan, *ACS Omega* **2021**, *6*, 23837–23845.
[10] I. Ahmed, *Arab J. Nucl. Sci. Appl.* **2021**, *54*, 50–62.
[11] J. Lin, Y. Zhang, Q. Zhang, J. Shang, F. Deng, *Environ. Sci. Pollut. Res. Int.* **2021**, *28*, 48236–48252.
[12] L. J. Foruzin, Z. Rezvani, *Mater. Chem. Phys.* **2021**, *267*, 124716.
[13] Q. Wang, J. Wu, Y. Gao, Z. Zhang, J. Wang, X. Zhang, X. Yan, A. Umar, Z. Guo, D. O'Hare, *RSC Adv.* **2013**, *3*, 26017–26024.
[14] L. J. Foruzin, Z. Rezvani, K. Nejati, *J. Iran. Chem. Soc.* **2018**, *15*, 2649–2658.

[15] E. M. Moujahid, R. Lahkale, H. Ouassif, F. Bouragba, W. Elhatimi, *Dyes Pigm.* **2019**, *162*, 998–1004.
[16] S. Sanati, Z. Rezvani, *J. Mol. Liq.* **2018**, *249*, 318–325.
[17] S. Samuei, F. A. Rad, Z. Rezvani, *Appl. Clay Sci.* **2020**, *184*, 105388.
[18] J. A. Bhojaraj, M. R. Kolinjavadi, M. Rajamathi, *ACS Omega* **2019**, *4*, 20072–20079.
[19] L. Yan, Y. Wang, J. Li, S. Kalytchuk, A. S. Susha, S. V. Kershaw, F. Yan, A. L. Rogach, X. Chen, *J. Mater. Chem. C* **2014**, *2*, 4490–4494.
[20] a) R. Sasai, H. Miyanaga, M. Morita, *Clay Sci.* **2013**, *17*, 35–40; b) R. Sasai, T. Itoh, W. Ohmori, H. Itoh, M. Kusunoki, *J. Phys. Chem. C* **2009**, *113*, 415–421.
[21] W. Shi, Z. Sun, M. Wei, D. G. Evans, X. Duan, *J. Phys. Chem. C* **2010**, *114*, 21070–21076.
[22] Z. Rezvani, L. J. Foruzin, K. Nejati, *J. Mol. Struct.* **2022**, *1274(1)*, 134555.
[23] G. Xia, Y. Zheng, Z. Sun, S. Xia, Z. Ni, J. Yao, *Environ. Sci. Pollut. Res. Int.* **2022**, *29*, 39441–39450.
[24] L. Jafari Foruzin, Z. Rezvani, K. Nejati, Z. Hou, H. Dai, K. Asadpour-Zeynali, *J. Mol. Liq.* **2019**, *288*, 111035.
[25] B. Zhang, Z. Dong, D. Sun, T. Wu, Y. Li, *J. Ind. Eng. Chem.* **2017**, *49*, 208–218.
[26] S. Gago, T. Costa, J. Seixas de Melo, I. S. Gonçalves, M. Pillinger, *J. Mater. Chem.* **2008**, *18*, 894–904.
[27] M. Salem, J. Salem, H. Ghannam, I. Massoudi, F. Bourguiba, M. Gaidi, *J. Mater. Sci.* **2023**, *34*, 332.
[28] Z. Sun, L. Jin, W. Shi, M. Wei, X. Duan, *Chem. Eng. J.* **2010**, *161*, 293–300.
[29] P. Tang, Y. Feng, D. Li, *Dyes Pigm.* **2011**, *90*, 253–258.
[30] Z. Xu, H. Zeng, *Chem. Mater.* **2001**, *13*, 4564–4572.
[31] S. Yu, J. Liu, W. Zhu, Z.-T. Hu, T.-T. Lim, X. Yan, *Sci. Rep.* **2015**, *5*, 1–12.
[32] R. K. Sonker, B. Yadav, V. Gupta, M. Tomar, *Mater. Chem. Phys.* **2020**, *239*, 121975.
[33] F. Chang, X. Wang, C. Yang, S. Li, J. Wang, W. Yang, F. Dong, X. Hu, D.-g. Liu, Y. Kong, *Composites Part B* **2022**, *231*, 109600.
[34] D. Yan, J. Lu, M. Wei, J. Ma, D. G. Evans, X. Duan, *Phys. Chem. Chem. Phys.* **2009**, *11*, 9200–9209.
[35] S. Samuei, J. Fakkar, Z. Rezvani, A. Shomali, B. Habibi, *Anal. Biochem.* **2017**, *521*, 31–39.
[36] R. Liang, S. Xu, D. Yan, W. Shi, R. Tian, H. Yan, M. Wei, D. G. Evans, X. Duan, *Adv. Funct. Mater.* **2012**, *22*, 4940–4948.
[37] Z. Meng, K. Fu, Y. Zhao, Y. Zhang, Z. Wei, Y. Liu, X.-K. Ren, Z.-Q. Yu, *J. Mater. Chem. C* **2020**, *8*, 1010–1016.
[38] J. Zhao, Y. Lu, D. Wu, Y. Qin, Y. Xie, Y. Guo, W. Raza, G. Luo, M. A. Mushtaq, Y. Wu, *Sep. Purif. Technol.* **2023**, *305*, 122508.

Manuscript received: February 17, 2023